Available online at www.sciencedirect.com
SCIENCE DIRECT
Powder Technology 161 (2006) 145 – 149
POWDER TECHNOLOGY
www.elsevier.com/locate/powtec

Effect of water of crystallization on synthesis of nanocrystalline ceria by non-hydrolytic method

M. Kamruddin *, P.K. Ajikumar, R. Nithya, G. Mangamma, A.K. Tyagi, Baldev Raj

Metallurgy and Materials Group, Indira Gandhi Centre for Atomic Research, Kalpakkam, India

Received 14 March 2005; received in revised form 23 September 2005; accepted 13 October 2005
Available online 2 December 2005

Abstract

Nanocrystalline ceria has been synthesized by a non-hydrolytic method using organic solvent and precipitant. The effect of the source compound on final nanocrystalline powder was investigated. The cerium nitrate hexahydrate subjected to different vacuum/thermal treatments to get cerium source compound having different extent of water of crystallization. The nanoceria, synthesized from these compounds was characterized by TGA-MS, XRD, HR-TEM and AFM.

Keywords: Nanocrystalline materials; Ceria; Non-hydrolytic synthesis; AFM; TGA-MS

1. Introduction

Nanocrystalline rare-earth oxides show vastly different optical and electronic properties compared to their microcrystalline counterparts. Their physical properties can be greatly influenced by particle size and synthesis methods. This has attracted a lot of research interest in the last few years [1,2]. Ceria (CeO_2) is an important rare-earth oxide with rapidly increasing applications in several fields due to its high refractive nature, strong UV absorption property and high transparency in the visible and IR region [3]. It is a potential electrolyte material for intermediate temperature SOFC due to its high oxygen ion conductivity and low cost. It is also used as gas sensors, oxygen pumps [4], catalytic support and promoter for heterogeneous catalytic reactions, coatings for high temperature applications [5] and as a surrogate material for studies of thermo-physical properties of actinide based oxides (ex. PuO_2) [6]. Nanocrystalline nature has also attracted attention as it provides faster densification kinetics, lower sintering temperature, finer microstructure and better property of sintered material [7].

These wide ranging applications have generated large research interest on synthesis of nanoceria by methods like hydrothermal, sol-gel, homogeneous precipitation, spray pyrolysis, sonochemical and microwave heating [4,8–12] for size control and better powder properties. The nanoparticles obtained from these hydrolytic processes contain hydroxyl groups on their surface which can affect the materials property [13]. These particles also tend to form hard agglomerates due to bridging of adjacent particles by hydrogen bonding and subsequent drying leading to huge capillary forces between particles [14]. Hence, these hydroxyl groups need to be replaced by other functional groups or eliminated by high temperature sintering which imposes main challenge to take full advantage of nanocrystalline materials. A better solution to this problem is non-hydrolytic method using organic solvents instead of water as nucleophilic agent [13]. The twin advantage of this method is that the organic solvent acts as a dispersant for solid particles during precipitation and also prevent them from aggregating during drying [14]. Nanocrystalline ZrO_2 and CeO_2 were synthesized by solvothermal process [15,16]. The effect of different alcohols on crystal structure, size and morphologies of nanocrystalline TiO_2 and CeO_2 were also investigated [13,14]. However, to the best of our knowledge, the effect of water of crystallization of cerium source compound on nanoceria product has not been studied. In the present work, nanoceria has been synthesized from cerium

* Corresponding author.
E-mail address: aji@igcar.ernet.in (M. Kamruddin).

0032-5910/$ - see front matter © 2005 Elsevier B.V. All rights reserved.
doi:10.1016/j.powtec.2005.10.003

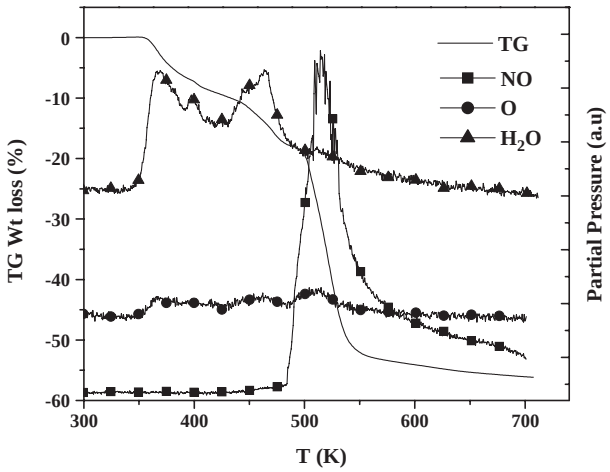

Fig. 1. TGA-MS spectra of V-RT compound.

nitrate hexahydrate (CeN) by soft-chemistry method using an organic solvent and organic precipitant. It is also aimed to study the effect of water of crystallization of cerium source compound on nanoceria product. Nanoceria synthesized by vacuum decomposition of CeN, which does not involve any solution, was used for comparison. The synthesis reaction was characterized by Thermogravimetry-Mass Spectrometry and nanocrystalline products were characterized by XRD, HR-TEM and Atomic Force Microscopy (AFM).

2. Experimental

The materials used are analytical grade cerium(III) nitrate hexahydrate, (Fluka), absolute ethanol (Hayman, England) and diethylamine (DEA) (S.d.fine-Chem., India) without any further purification. The cerium source compounds prepared for this study are (1) raw CeN (R), (2) CeN vacuum (10^{-5} mbar) treated at RT for 12 h (V-RT), (3) CeN vacuum treated at 425 K for 12 h (V-425) and (4) CeN vacuum treated at 500 K for 12 h (V-500). The first three compounds were used for synthesizing the solvated precursor by non-hydrolytic method and the fourth for synthesis of nanoceria for comparison by Temperature Programmed Decomposition (TPD) method.

For the non-hydrolytic method, the stock solutions were prepared by dissolving the cerium compounds (1 to 3) in abs. ethanol (0.1 M) and DEA in abs. ethanol (1.0 M). The precipitation reaction was carried out at RT by slow addition of DEA solution to cerium stock solution under constant stirring. After addition, the mixtures were refluxed at 323 K for 30 min. The resulted pale yellow precipitate was separated by vacuum filtration, washed thrice with alcohol and dried overnight at 350 K. These precursors and V-500 sample were then decomposed to get the final nanoceria powder. These conversion reactions were studied by tracking the sample mass variation and concentration of product gases in an indigenously assembled Thermogravimetry-Evolved Gas Analysis by Mass Spectrometry (TGA-MS) system [17]. The characterization of the solvated precursors and the nanoceria powders was done using an X-ray powder diffractometer (STOE) with Cu K_α radiation at a scan rate in 2θ of 0.05°/7 s in the angular range 20–80°. The hygroscopic cerium compounds were loaded in a 0.5 mm Lindemann capillary in an inert atmosphere glove box and capped with wax. Bright field electron micrographs and selected area diffraction (SAD) were obtained using a TEM (JEOL JEM 2010 Electron Microscope, 200 kV). The nanocrystalline powders were dispersed in alcohol by ultrasonification and a drop of this solution was placed on a holey carbon film held on a copper grid for TEM analysis. The topography of uniaxially pressed green pellets were obtained using a Solver PRO, Scanning Probe Microscope (M/s. NT-MDT, Russia).

3. Results and discussion

3.1. TPD of vacuum precursors

Earlier mass spectrometry investigation of TPD of CeN [18] has shown that the dehydration occurs through sequential but overlapped steps spanning up to 510 K. It suggests the crystallographic inequivalence in the water molecules around the metal atom. As in the case of thorium nitrate pentahydrate, in CeN also, the cerium metal is coordinated to six oxygen atoms of three bidentate nitrate groups and to one oxygen atom each of five water molecules and drives a coordination no. 11 [19]. The last water molecule resides outside the coordination sphere. Thus it is clear that these water molecules may be removed in parts by appropriate vacuum/thermal treatment.

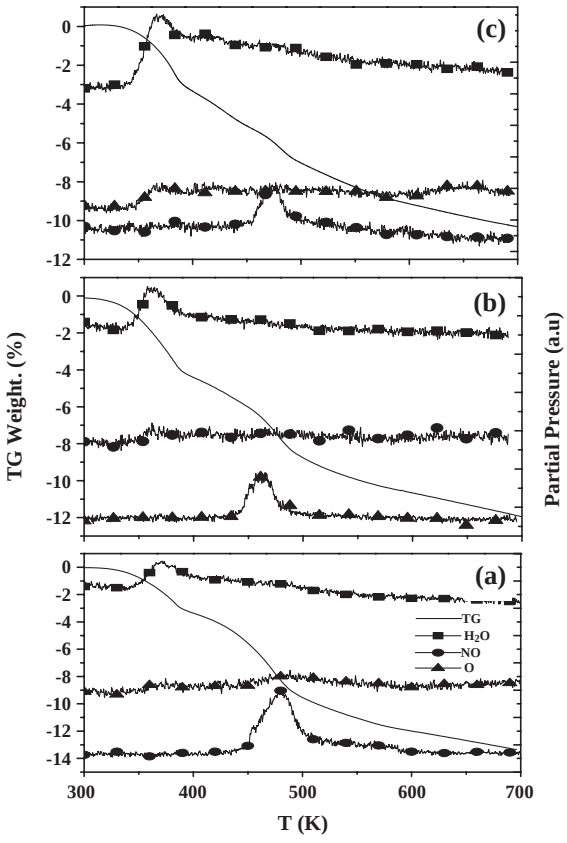

Fig. 2. The TGA-MS spectra showing the TG weight change and MS signal of compounds (a) R, (b) V-RT and (c) V-425.

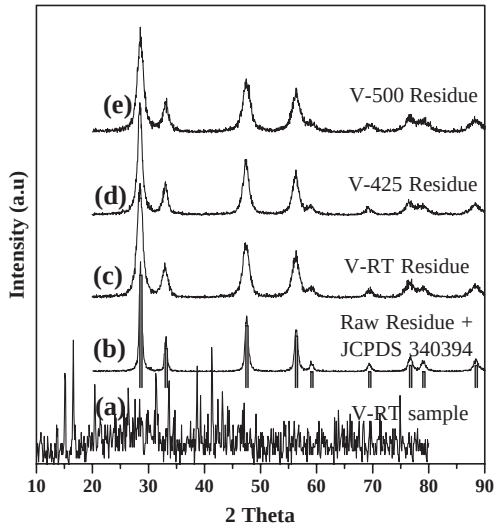

Fig. 3. XRD patterns of Ce compounds and nanoceria with corresponding JCPDS data.

The denitration reaction, which starts well before the completion of dehydration, occurs in the temperature range 475–780 K. Hence, the temperatures for vacuum treatment were fixed as follows: 1) RT to remove the more labile water, 2) 425 K to remove maximum number of water molecules without effecting any decomposition of nitrate salt and 3) 500 K to prepare ceria by TPD for comparison.

A typical TGA-MS spectra of TPD of V-RT sample, at 4 K/min, giving the weight loss and product gas release profiles (of H_2O, O and NO) are shown in Fig. 1. The mass spectrometry (MS) signal of H_2O and NO releases indicate that the initial poorly resolved weight loss of 18.5% is due to dehydration followed by 34% loss for nitrate decomposition. Further a weight loss of ~4.5% beyond 550 K is due to decomposition of residual nitrate. These weight losses suggest that V-RT compound is pentahydrate (which is also confirmed by XRD).

Similar exercise on TPD of V-425 sample showed weight losses of around 4%, 41% and 4% corresponding to dehydration, denitration and decomposition of residual nitrates, respectively. The 4% weight loss of dehydration suggest that the starting compound is cerium nitrate monohydrate. In both these cases, the overall weight loss indicated formation of CeO_2 as final product.

3.2. TPD of solvated precursors

The precursors obtained from vacuum treated starting materials were also subjected to TPD and the reactions leading to formation of nanoceria were studied by TGA-MS (Fig. 2a,b and c). The figures show the TG weight loss along with the corresponding MS gas release profiles. All the precursors show a four stage decomposition. The first two were due to dehydration, third and fourth were due to decomposition of parent nitrate compound. As observed earlier [18], even repeated washes do not remove the parent nitrate completely. The weight losses observed in these samples due to dehydration are 5.3%, 5.0% and 4.2% and due to decomposition of nitrate are 8.8%, 7.6% and 6.4% for R, V-RT and V-425, respectively. This clearly shows that the extent of hydration of the starting compound affects the precursor. The higher water content of starting material produced more hydrolysed precursor and it also dissolved and carried more parent nitrate to the precursor. The overall weight losses indicate formation of ceria.

3.3. XRD investigations

The XRD pattern of the starting compound, V-RT is shown in Fig. 3a. By comparing with diffraction data (JCPDS No. 220544) it was found to be mostly cerium nitrate pentahydrate. However, the V-425 which has been identified as cerium nitrate monohydrate by TG weight loss could not be ascertained as there was no corresponding diffraction data available. The XRD patterns of all nanoceria synthesized from different precursors (shown in Fig. 3b,c,d and e) were identical and could be indexed to the standard CeO_2 with fluorite structure (JCPDS 340394). The peaks were considerably broader due to the smaller crystallite size and perhaps contribution from lattice microstrain. From the peak width analysis using integral breadth method, the microstructural parameters namely, size and lattice strain were determined [18]. The WinXPOW software of STOE was used to fit diffraction profiles and extract the peak position, FWHM and integral breadth. After subtracting the instrument broadening (obtained from the NIST standard CeO_2), the Williamson–Hall method was used to determine strain and crystallite size. This analysis has shown that the R sample yielded nanoceria with largest particle size, a smaller particle size for methods V-RT and V-425 and smallest for V-500 compound. The strain in the nanoceria samples was found to be in the range of $2-5*10^{-3}$ showing an inverse relation with particle size. These values are given in Table 1. The particle sizes were also determined by HR-TEM.

The refined lattice parameters of these nanocrystalline ceria were determined using Werner's algorithm and compared with the lattice parameter(a_o) of 5.4117 Å for NIST standard ceria. All the samples showed lattice dilation with a maximum by V-

Table 1
Weight change, particle size (nm), strain and state of agglomeration of nanoceria

Sample ID	Wt. change (%)		Particle size		Strain $\times 10^3$	AFM	
	Dehydration	Denitration	XRD	TEM		Size	Agglomeration state
Raw	5.3	8.0	21.4	20–30	2.2	<50	Large agglomerates
V-RT	5.0	7.5	10.8	10–15	3.1	<30	Small agglomerates
V-425	4.2	6.4	11.2	7–11	5.2	<20	Agglomerate free
V-500	–	–	7.8	5–8	4.8	<20	-do-

425 sample ($a=5.4206$ Å; $\Delta a/a_o=0.16\%$). However, no systematic variation with particle size or preparation method was observed.

The increase in lattice parameter can be attributed to formation of trivalent metal and associated oxygen vacancy [20]. The formation of xCe^{3+} and the oxygen ion vacancy V_o can be written as:

$$CeO_2 \leftrightarrow Ce^{4+}_{1-x}Ce^{3+}_{x}O^{2-}_{2-\frac{x}{2}}\cdot\left(\frac{x}{2}\right)V_o + \left(\frac{x}{4}\right)O_2 \quad (1)$$

For such a system the lattice parameter "a" can be written as: $a(x)=(4/\sqrt{3})[r_{\text{cation}}-r_{\text{anion}}]$, where x is the molefraction of Ce^{3+} (or $\simeq Ce^{3+}$ to Ce^{4+} ratio) and r_{cation} and r_{anion} are the effective radii of cation and anion, respectively.

$$a(x) = \frac{4}{\sqrt{3}}\left[xr_{3+} - (1-x)r_{4+} + \left(1-\frac{x}{4}\right)r_o + \frac{x}{4}r_{vo}\right] \quad (2)$$

where r_{3+} and r_{4+} are the radii of cerium 3+ and 4+ ions, respectively, r_o and r_{vo} are the radii of oxygen ion and oxygen vacancy, respectively. Eq. (2) can be rewritten to show the linear dependence of "a" on x as:

$$a(x) = \frac{4}{\sqrt{3}}\left[r_3 - r_4 - \frac{r_o}{4} + \frac{r_{vo}}{4}\right]x + \frac{4}{\sqrt{3}}[r_{4+} + r_o] \quad (3)$$

and one can write that $[Ce^{3+}]=2[V_o]$ and $[Ce^{3+}]/[O_2]=x/4$. Using the observed change in lattice parameter, the oxygen vacancy concentrations were calculated for the nanoceria samples [18] using the above formalism and found to be in the range of $2.5-4\times10^{20}/cm^3$.

3.4. HR-TEM investigations

The size and shape of the nanoceria particles and their degree of agglomeration were obtained by HR-TEM. The brightfield micrographs and the corresponding SAD patterns (inset) of nanoceria obtained by non-hydrolytic method and TPD are shown in Fig. 4a,b,c and d. All the methods yielded more or less spherical particles with relatively narrow size distribution. However, their sizes and states of agglomeration were different. Fig. 4a shows that the size of the particles obtained from R precursor is in the range of 20–30 nm and they are fairly agglomerated. Their larger size is also evident from the spotty rings of SAD pattern. Fig. 4b shows that the nanoceria obtained from V-RT precursor is of smaller size (10–15 nm) but still contained loose agglomerates. The rings in the SAD pattern were fairly complete and less spotty. Fig. 4c and d show that the nanoceria synthesized from V-425 and by TPD were of still smaller sizes (7–11 and 5–8 nm, respectively) and were dispersed. The rings in the SAD patterns were also more continuous and less spotty. All the SAD patterns could be indexed (not shown) to various planes of standard fluorite ceria. Except for a lower size of V-RT obtained by XRD, the particle sizes determined by XRD and TEM match well (Table 1).

3.5. AFM investigations

Having determined the sizes by XRD and HR-TEM, we have also attempted to get the particle sizes and the degree of agglomeration by AFM. Green pellets (dia. 5 mm and thickness ~1 mm) of nanocrystalline powders were used to obtain the topography. The contact mode, where the tip of the AFM cantilever is in physical contact with sample and rastered to get topography, is a better mode to observe such small features. However, it was found that green pellets were not suitable for this mode as nanocrystalline powders were sticking to the tip. Hence, semi-contact or non-contact mode was used to obtain the topography of the pellets. The cantilever used in this study was a Au coated Si with force constant ~11 N/m and having a tip radius ~10 nm. Hence, features below 20 nm and thus the particle sizes were not probed. However, the AFM investigation is mainly used to verify the extent of agglomeration. The surface topography of these pellets is shown in Fig. 5a,b,c and d.

Fig. 5a shows that the ceria obtained from R-sample consisted of large agglomerates of sizes 150–200 nm. The topography of nanoceria (Fig. 5b) obtained from V-RT precursor shows lesser agglomeration. Fig. 5c and d shows much finer features and almost void of any agglomeration. These observations matched well with HR-TEM results.

While all other conditions being the same, the only difference w.r. to final ceria is the extent of water of crystallization of the starting cerium source compound. Hence,

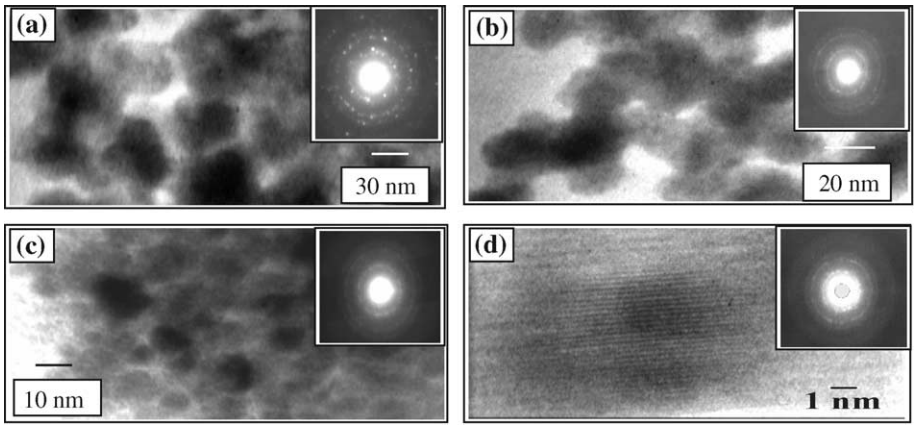

Fig. 4. TEM images and SAD patterns of nanoceria prepared from (a) R (b) V-RT (c) V-425 and (d) V-500 samples.

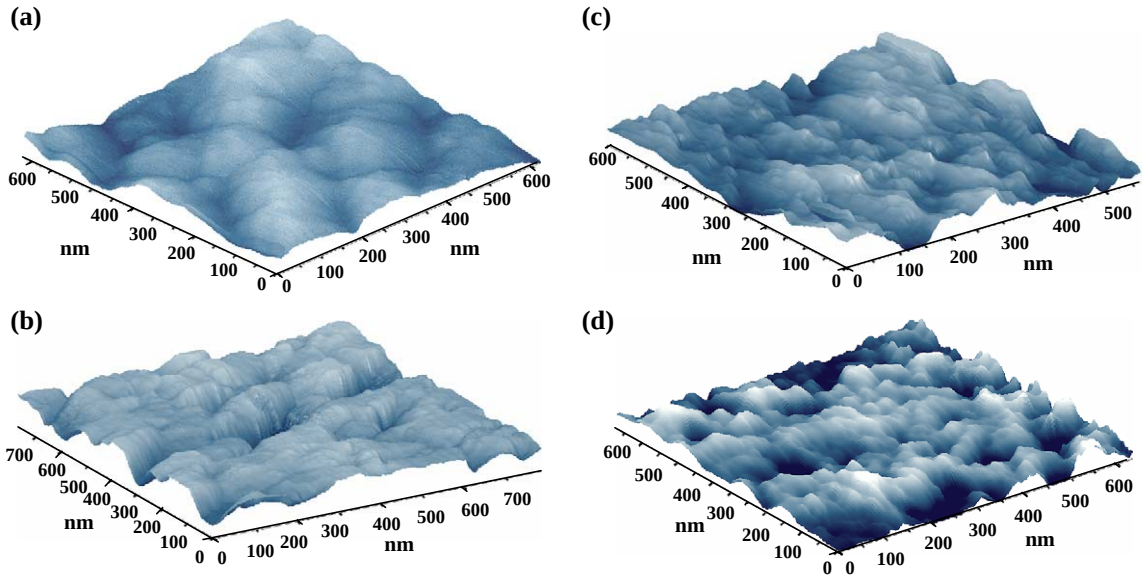

Fig. 5. AFM topographies of nanoceria prepared from (a) R (b) V-RT (c) V-425 and (d) V-500.

the changes observed in the nanoceria can be ascribed to this effect which in turn is expected to alter hydrogen bonding. Moreover, the TGA-MS data has clearly indicated a direct relationship between the water content of the starting compound to the hydrolysed nature of the precursor. Hence, from the above results it is clear that the water of crystallization of cerium source compound has an effect on final nanoceria product. The R-sample having maximum number of water of crystallization (i.e. $6H_2O$) is expected to offer maximum hydrogen bonding. Thus the nanoceria obtained from this sample were of larger size and highly agglomerated. However, the V-RT sample with around $5H_2O$ produced considerably smaller size particles suggesting that the removal of the more labile water molecule lying outside the coordination sphere reduces the hydrogen bonding between the particles considerably. The third sample V-425, where four out of five water molecules connected to Ce metal were removed, produced nanoceria having sizes slightly smaller than V-RT substantiates the above observation. However, having considerably less water molecules produced agglomeration free nanoceria. Moreover, the carryover of parent nitrate in precursors is also less. The non-hydrolytic method produced particles with lower strain and they followed the expected inverse relation with particle size.

4. Conclusion

Fine nanoceria powders were synthesized by non-hydrolytic method. TGA-MS results on TPD of CeN are utilized to arrive at appropriate thermal treatments to prepare the starting cerium compounds with different extent of water of crystallization. The compounds thus prepared were hydrolysed by a non-hydrolytic method in alcohol medium using diethylamine. Water of crystallization of the starting cerium source compound is found to have an effect on the size, extent of agglomeration of nanocrystalline particles and on the carry over of parent nitrate compound. Absence of water and thus bridging hydrogen bonding between adjacent particles explains the smaller size and lesser agglomeration in nanoceria prepared from V-425 precursor which is comparable to nanoceria obtained by solvent free decomposition method.

Acknowledgement

The authors are thankful to Dr. Satyam PV and Shri. Joy Gatak of IOP, Bhubaneswar for HR-TEM investigations.

References

[1] F. Zhang, S.W. Chan, J.E. Spanier, Ebru Apak, Q. Jin, R.D. Robinson, I.P. Herman, Appd. Phys. Lett. 80 (2002) 127.
[2] W.J. Li, E.W. Shi, T. Fukuda, Cryst. Res. Technol. 38 (2003) 847.
[3] D. Berreca, G. Bruno, A. Gasparotto, M. Losurdo, E. Tondello, Mater. Sci. Eng., C, Biomim. Mater., Sens. Syst. 23 (2003) 1013.
[4] M.S. Tsai, Mater. Sci. Eng., B, Solid-State Mater. Adv. Technol. 110 (2004) 132.
[5] F. Czerwinski, J.A. Szpunar, J. Sol-Gel Sci. Technol. 9 (1997) 103.
[6] C. Degueldre, J.M. Paratte, J. Nucl. Mater. 274 (1999) 1.
[7] Y. Zhou, M.N. Rahaman, Acta Mater. 45 (1997) 3635.
[8] M. Hirano, E. Kato, J. Am. Ceram. Soc. 79 (1996) 777.
[9] N.B. Kirk, J.V. Wood, J. Mater. Sci. 30 (1995) 2171.
[10] B. Djuricic, S. Pickering, J. Eur. Ceram. Soc. 19 (1999) 1925.
[11] L. Madler, W.J. Stark, S.E. Pratsinis, J. Mater. Res. 17 (2002) 1356.
[12] H. Wang, J.J. Zhu, J.M. Zhu, X.H. Liao, S. Xu, T. Ding, H.Y. Chen, Phys. Chem. Chem. Phys. 4 (2002) 3794.
[13] C. Wang, Z.X. Deng, G. Zhang, S. Fan, Y. Li, Powder Technol. 125 (2002) 39.
[14] J.G. Li, T. Ikegami, J.H. Lee, T. Mori, Acta Mater. 49 (2000) 419.
[15] J. Zhao, W. Fan, D. Wu, Y. Sun, J. Mater. Res. 15 (2000) 402.
[16] Y.W. Zhang, R. Si, C.S. Liao, C.H. Yan, C.X. Xiao, Y. Kou, J. Phys. Chem., B 107 (2003) 10159.
[17] M. Kamruddin, P.K. Ajikumar, S. Dash, A.K. Tyagi, B. Raj, Bull. Mater. Sci. 26 (2003) 449.
[18] M. Kamruddin, P.K. Ajikumar, R. Nithya, A.K. Tyagi, B. Raj, Scr. Mater. 50 (2004) 417.
[19] T. Ueki, A. Zalkin, D.H. Templeton, Acta Crystallogr. 20 (1966) 836.
[20] J. Zhang, Z.C. Kang, L. Eyring, J. Alloys Compd. 192 (1993) 57.